Molecular Cell
Article

Molecular Mechanism of Sequence-Directed DNA Loading and Translocation by FtsK

Jan Löwe,[1,*] Antti Ellonen,[2] Mark D. Allen,[3] Claire Atkinson,[2] David J. Sherratt,[2] and Ian Grainge[2,*]
[1]MRC Laboratory of Molecular Biology, Hills Road, Cambridge CB2 0QH, UK
[2]Department of Biochemistry, University of Oxford, Oxford OX1 3QU, UK
[3]Centre for Protein Engineering, MRC, Hills Road, Cambridge CB2 0QH, UK
*Correspondence: jyl@mrc-lmb.cam.ac.uk (J.L.), ian.grainge@bioch.ox.ac.uk (I.G.)
DOI 10.1016/j.molcel.2008.05.027

SUMMARY

Dimeric circular chromosomes, formed by recombination between monomer sisters, cannot be segregated to daughter cells at cell division. XerCD site-specific recombination at the *Escherichia coli dif* site converts these dimers to monomers in a reaction that requires the DNA translocase FtsK. Short DNA sequences, KOPS (GGGNAGGG), which are polarized toward *dif* in the chromosome, direct FtsK translocation. FtsK interacts with KOPS through a C-terminal winged helix domain γ. The crystal structure of three FtsKγ domains bound to 8 bp KOPS DNA demonstrates how three γ domains recognize KOPS. Using covalently linked dimers of FtsK, we infer that three γ domains per hexamer are sufficient to recognize KOPS and load FtsK and subsequently activate recombination at *dif*. During translocation, FtsK fails to recognize an inverted KOPS sequence. Therefore, we propose that KOPS act solely as a loading site for FtsK, resulting in a unidirectionally oriented hexameric motor upon DNA.

INTRODUCTION

Investigations of the bacterial chromosome are revealing ever more intricate levels of control in its organization and segregation (reviewed in Draper and Gober, 2002; Ebersbach and Gerdes, 2005; Ghosh et al., 2006; Sherratt, 2003). FtsK is a DNA translocase, highly conserved across bacteria, that plays a role in the later stages of cell division and chromosome segregation. It is localized to the developing septum by interaction with FtsZ, and, once there, the motor domain can translocate on DNA that is present in the region of the septum. This occurs when there has not been a timely separation of replicated chromosomes, for example, when chromosome catenanes or dimers are present. FtsK translocation then directs the topologically simple synapsis of the sister *dif* sites bound by XerC and XerD. Recombination is stimulated directly by FtsK until daughter chromosomes are unlinked (Grainge et al., 2007). Remarkably, FtsK is able to "read" the sequence of the DNA to determine its direction of movement so that its net movement should always be toward the *dif* site (for recent reviews, see Bigot et al., 2007; Strick and Quessada-Vial, 2006).

FtsK is a member of the FtsK/SpoIIIE/Tra family of DNA translocases. SpoIIIE is required for the complete transfer of the chromosome into the prespore of sporulating bacteria (Wu et al., 1995) and was the first protein of this family to be identified as a DNA motor protein (Bath et al., 2000). Tra proteins are encoded by conjugative elements and are thought to pump DNA during bacterial conjugation (Gunton et al., 2007). *Escherichia coli* FtsK is a 1329 amino acids protein that consists of several domains. The N-terminal domain ($FtsK_N$) of about 200 residues contains four transmembrane helices (Dorazi and Dewar, 2000) and is part of the divisome, the multiprotein complex that orchestrates bacterial cell division (reviewed in Goehring and Beckwith, 2005; Vicente and Rico, 2006). It has been suggested that the N terminus of SpoIIIE may form a channel for DNA through the cell membrane, and a similar role could be envisaged with FtsK (Liu et al., 2006). This idea is supported by the similarity of some Tra proteins involved in conjugative transfer to the N-terminal domain of FtsK (Gunton et al., 2007).

Separating the N- and C-terminal domains of FtsK is a linker region ($FtsK_L$) that is ~600 residues long in *E. coli* and has a precise function that is unclear (Bigot et al., 2004). Following the linker is the DNA translocase $FtsK_C$, containing the αβ motor, followed by the 85 amino acid FtsKγ domain. The structure of FtsKαβ from *Pseudomonas aeruginosa* shows a hexamer that assembles around double-stranded DNA (Massey et al., 2006). The fold of the α domain is unique to the FtsK/SpoIIIE/Tra family, whereas β has a RecA-like fold common to a large number of helicases and other hexameric proteins such as AAA+ proteins (Iyer et al., 2004). Based on an observed conformational change, a "rotary inchworm" mechanism has been proposed (Massey et al., 2006) that explains the very fast translocation of FtsK on DNA with very little supercoiling induction (1/150 bp), as observed in "single-molecule" experiments (Saleh et al., 2005). In this mechanism, ATP hydrolysis by one of the six subunits of the FtsK ring translocates ~2 bp of DNA, bringing the helical backbone of the DNA into position for translocation by the next subunit in the ring. Thus, very little net rotation of the protein ring against the DNA is required, and this may aid the very high translocation speeds of 5 kbp/s observed in single-molecule experiments (Pease et al., 2005; Saleh et al., 2004).

FtsK has created great interest not only because of its prodigious speed of translocation but because its movement on DNA is directed toward *dif* by polarized sequences on the

chromosome (Corre and Louarn, 2002). Subsequent single-molecule experiments suggested that FtsK appeared to read the sequence of DNA while translocating (Pease et al., 2005). The sequence that imparts this directionality has the consensus 5′-GGGNAGGG-3′ and is termed FtsK Orienting Polarized Sequence (KOPS) (Bigot et al., 2005; Levy et al., 2005). KOPS is recognized directly by the FtsKγ domain (Ptacin et al., 2006; Sivanathan et al., 2006), which has a winged helix fold, as determined by NMR. The FtsKγ domain is also the site of interaction with XerD, and, thus, it is required for the activation of recombination (Yates et al., 2006). Further, it has been determined that the γ domains help with loading of the motor hexamer (αβ domains) on one side of the KOPS sequences only (Bigot et al., 2006). Yet, it has been unclear how KOPS is recognized in the whole complex of the α, β, and γ domains and how γ apparently recognizes KOPS in the "permissive" orientation to load a hexamer and in the opposite "nonpermissive" orientation to pause/reverse a hexamer.

Here, we report a high-resolution crystal structure of three FtsKγ domains bound to KOPS. The structure shows three γ domains recognizing the 8 bp KOPS with sequence specificity, employing two different DNA-binding modes as well as protein-protein interactions. Using covalent dimeric $FtsK_C$ proteins, we show that three γ domains per hexamer are sufficient for KOPS recognition and recombination at *dif*. Importantly, we demonstrate that FtsK does not recognize KOPS in the nonpermissive orientation; a translocating hexamer passes through these sequences. Instead, the KOPS-γ interaction yields a FtsK hexamer loaded onto DNA in a defined orientation on one side of KOPS. Therefore, we believe the biological role of KOPS is most likely purely a loading mechanism for correctly orienting FtsK on DNA prior to translocation.

RESULTS AND DISCUSSION

The FtsKγ Domain Is a Winged-Helix Domain

We have crystallized the FtsKγ domain from *Pseudomonas aeruginosa* and solved the structure to 1.4 Å resolution by molecular replacement using the NMR structure determined by us previously (Sivanathan et al., 2006; Tables 1 and 2). The new high-resolution structure confirms that FtsKγ is a winged helix domain (WHD) (Figure S1A available online). The WHD fold is comprised of helices H1 to H3 and a wing that is in β sheet-like conformation, though the new high-resolution crystal structure shows that the two strands do not have a regular β sheet hydrogen-bonding network between them. Estimation of the electrostatic potential on the surface of the domain, which can now be performed to a greater precision, identifies a patch of positive charge, mostly around the loop between helices H2 and H3 (Figure S1B). Surprisingly, the crystals contained eight molecules per asymmetric unit (Figure S1C). These are arranged in a tight octamer with 222 symmetry. The structure is very compact, with between ~1600 $Å^2$ and ~1300 $Å^2$ buried (26%–34% of the monomer surface) for the different positions in the octamer. There is currently no evidence that this arrangement has any biological significance, and it is not related to the packing when bound to DNA (described below), though it is tempting to speculate that a similar self-interaction of γ domains in the absence of KOPS DNA might be part of its regulation.

Table 1. Crystallographic Data

Pseudomonas aeruginosa FtsK (FTSK_PSEAE) γ-Domain: GGS-742-811; P2(1), a = 44.5 Å, b = 58.5 Å, c = 95.4 Å, β = 92.5°

Crystal	λ [Å]	Resol.	I/σI[a]	Rm[b](%)	Multipl.[c]	Compl.(%)[d]
NATI	0.9393	1.4	13.1(3.0)	0.088(0.532)	4.0	99.9

Pseudomonas aeruginosa FtsK (FTSK_PSEAE) γ-Domain: GGS-742-811 with KOPS-Containing DNA Duplex: 5′-ACCAGGGCAGGGCGAC-3′; C2, a = 137.9 Å, b = 63.1 Å, c = 76.0 Å, β = 118.8°

Crystal	λ [Å]	Resol.	I/σI[a]	Rm[b](%)	Multipl.[c]	Compl.(%)[d]
PEAK	0.9796	1.9	23.3(3.8)	0.051(0.318)	6.7(3.3)	99.7
INFL	0.9798	2.2	32.1(14.3)	0.041(0.114)	7.3(3.7)	99.7
HREM	0.9687	2.2	29.1(10.7)	0.044(0.153)	7.3(3.8)	99.8

[a] Signal-to-noise ratio for merged intensities.
[b] Rm: $\Sigma h \Sigma i |I(h,i)–I(h)| / \Sigma h \Sigma i\, I(h,i)$, where I(h,i) are symmetry-related intensities and I(h) is the mean intensity of the reflection with unique index h.
[c] Multiplicity for unique reflections (anomalous multiplicity in brackets).
[d] Completeness for unique reflections. Highest resolution bins in brackets. The native structure was solved using molecular replacement using the NMR structure as search model (PDB ID 2J5O). The DNA cocrystal was solved using the SeMet MAD data set for phase determination. The CC of anomalous pairs for the peak data set was 0.15 to 2.2 Å resolution.

Three γ Domains Recognize One KOPS Sequence

In order to better understand how FtsKγ recognizes KOPS sequences, we cocrystallized the protein with 16 bp of double-stranded DNA containing the KOPS sequence, GGGCAGGG (Bigot et al., 2005; Ptacin et al., 2006). Bioinformatic studies have suggested that this same sequence is likely to be the KOPS sequence in *Pseudomonas aeruginosa* (Hendrickson and Lawrence, 2006), and this sequence was previously shown to be recognized by both *E. coli* and *P. aeruginosa* γ (Sivanathan et al., 2006). The structure was solved by SeMet MAD phasing to 1.9 Å resolution (Tables 1 and 2). The crystals contain two double-stranded DNA molecules bound by six FtsKγ domains; the complexes are arranged so that a unit containing three FtsKγ domains and one DNA is present twice (Figure 1A). The ends of the DNA are partly unwound and partly overlap. In the overlapping regions, Watson-Crick base pairs form between the different strands, though the DNA used is blunt-ended. The binding mode of one molecule of FtsKγ to DNA is shown in Figure 1B; the WHD domain makes many contacts with the major groove of the DNA, binding to the backbone as well as reading the base sequence. For this, the loop between helices H2 and H3 and one side of H2 insert into the groove, as was determined by nuclear magnetic resonance studies (NMR). The wing of the WHD interacts with the next minor groove, as is common for these domains (Gajiwala and Burley, 2000). When looking along the DNA (Figure 1C), the three domains follow the major groove and bind every 80°–100°, with the first and last being almost exactly 180° apart. When bound by the three domains, the DNA does not significantly change its conformation and is very close to ideal B-DNA (Figure 1D). We believe that this makes it unlikely that bending or non-B-DNA in KOPS bound by FtsKγ could somehow influence the FtsK motor.

Table 2. Refinement Statistics

Model	γ-Domain
	Eight protein chains A–H: A, 745–811; B, 745–809; C, 746–809; D, 744–811; E, 744–809; F, 744–808; G, 747–806; H, 747–808; 688 water molecules
Diffraction data	NATI, 50.0–1.4 Å, all data
R factor, R free[a]	0.14 (0.17), 0.19 (0.26)
B factors[b]	18.6 Å^2, 2.9 Å^2 (aniso)
Geometry[c]	0.030 Å, 2.33°
Ramachandran[d]	92.8%/0.0%
PDB ID	2VE8
Model	**γ-Domain: DNA Cocrystal**
	Two duplexes bound to three protein chains each: DNA chains I and J bound by protein chains A, B, and C; DNA chains K and L bound by protein chains D, E, and F; A, 746–807; B, 747–807; C, 746–807; I and J, 1–14; J, 1–16; D, 747–808; E, 747–808; F, 745–807; K, 1–14; L, 1–16; 510 water molecules, 1 Mg
Diffraction data	PEAK, 50.0–1.9 Å, all data
R factor, R free[a]	0.20 (0.27), 0.25 (0.36)
B factors[b]	40.3 Å^2, 1.15 Å^2
Geometry[c]	0.013 Å, 1.647°
Ramachandran[d]	94.1%/0.0%
PDB ID	2VE9

[a] 5% of reflections was randomly selected for determination of the free R factor prior to any refinement. R factors for the highest resolution bins are given in brackets.
[b] Temperature factors averaged for all atoms and RMS deviation of temperature factors between bonded atoms.
[c] RMS deviations from ideal geometry for bond lengths and restraint angles.
[d] Percentage of residues in the "most favored region" of the Ramachandran plot and percentage of outliers. All data were collected on beamline ID14eh4 (ESRF, Grenoble, France).

Cooperative Binding Enables the Recognition of Different Sequences by the Three FtsKγ Domains

One of the most interesting aspects of the complex structure between KOPS DNA and FtsKγ is the recognition of the DNA sequence, GGGCAGGG. To illustrate this, Figure 1E shows the three domains (A, B, and C) bound to the DNA, with color-coding highlighting the three parts of the sequence recognized by each. The first three Gs are recognized by subunit A (Figure 1E, left). The central C and A bases are recognized by the middle subunit B (Figure 1E, middle), and the last three Gs are recognized by subunit C (Figure 1E, right). Thus, subunits A and C recognize the same DNA sequence: GGG (Figure 1F). Accordingly, they also share exactly the same binding mode, with the wing of the WHD being inserted deep into the next minor groove. Subunit B is different. It recognizes a different sequence, is slightly tilted with the wing not so deeply penetrating the minor groove, and is generally further away from the DNA with many water molecules mediating contacts with the DNA (Figures 1E, middle, S1D, and S1E). This binding mode immediately explains why the KOPS consensus sequence is less stringent for positions four and five (Bigot et al., 2005) since these bases are not directly read by the protein. Table S1 provides a list of residues in γ that read the DNA sequence, notably S766, Q769, and N777, which make contacts to oxygens and nitrogens in the DNA bases via water molecules (Figure S2). These contacts are conserved between subunits A and C but are different in B. The binding modes of the three γ subunits also explain how a small domain such as FtsKγ can recognize such a large sequence motif. Most likely, subunits A and C bind to the GGG motifs of KOPS with higher affinity than subunit B to the CA motif, but cooperative interactions between the three γ domains stabilize the complex as a whole. Presumably, only three contributions to the binding energy are sufficient for effective binding of the B subunit: binding to DNA and protein-protein contacts with subunits A and C all at the same time. This cooperative binding mode enables the small FtsKγ WHD domain to recognize GGG and CA bases at the same time in a specific and ordered way. All three subunits bind in roughly the same orientation on the DNA (Figure 1F), orienting the N termini on one side of the complex and the C termini on the other. Importantly for this study, the orientation of the protein on the KOPS motif is such that all N termini of the FtsKγ domains point toward the 5′ end of the GGGCAGGG sequence.

A Model of KOPS-Directed Loading of the FtsK Motor Domain

Knowing the orientation of the γ domain on KOPS allows us for the first time to assemble a molecular model of FtsK, including the motor domains α and β, loaded in a specific orientation at KOPS (Figures 2A and 2B). Taking our previous model of FtsK bound to DNA (Massey et al., 2006), we orient it so that the C termini of the β domains join with the N termini of the γ domains. In unmodified FtsK, there is a short 10–14 amino acid linker between these two. This then places the motor on the 5′ side of the GGGCAGGG KOPS motif, which is in excellent agreement with previous data showing loading on the 5′ side of KOPS (Bigot et al., 2006). Our model also predicts that the motor moves so that the DNA enters the hexamer from β because we know which way around a KOPS sequence is permissive for translocation (Figure 2B). Interestingly, the three FtsKγ domains are not in angular register with the hexamers in the complex (Figure 2A). The significance of this is unknown, although the interaction with XerD and subsequent recombination might require this special arrangement in a way we currently do not understand. The model predicts that only three of the six FtsKγ subunits present are used for KOPS recognition. To confirm the structural data, we performed an isothermal titration calorimetry experiment (Figures 2C and 2D). We used the same double-stranded DNA as in the cocrystallization experiments and an unrelated DNA of the same length as negative control. The experiment yielded the same stoichiometry of ~3:1 protein:DNA as in the crystals described above. It is currently not possible to fit a suitable binding model for three subunits in order to obtain dissociation constants and binding energies. Possible roles of the three free γ domains in the complex bound to KOPS are discussed below.

If the model and predictions of directionality of the motor protein deduced here are correct, FtsKγ binding could interfere with translocation, because the KOPS-bound γ domains need to be

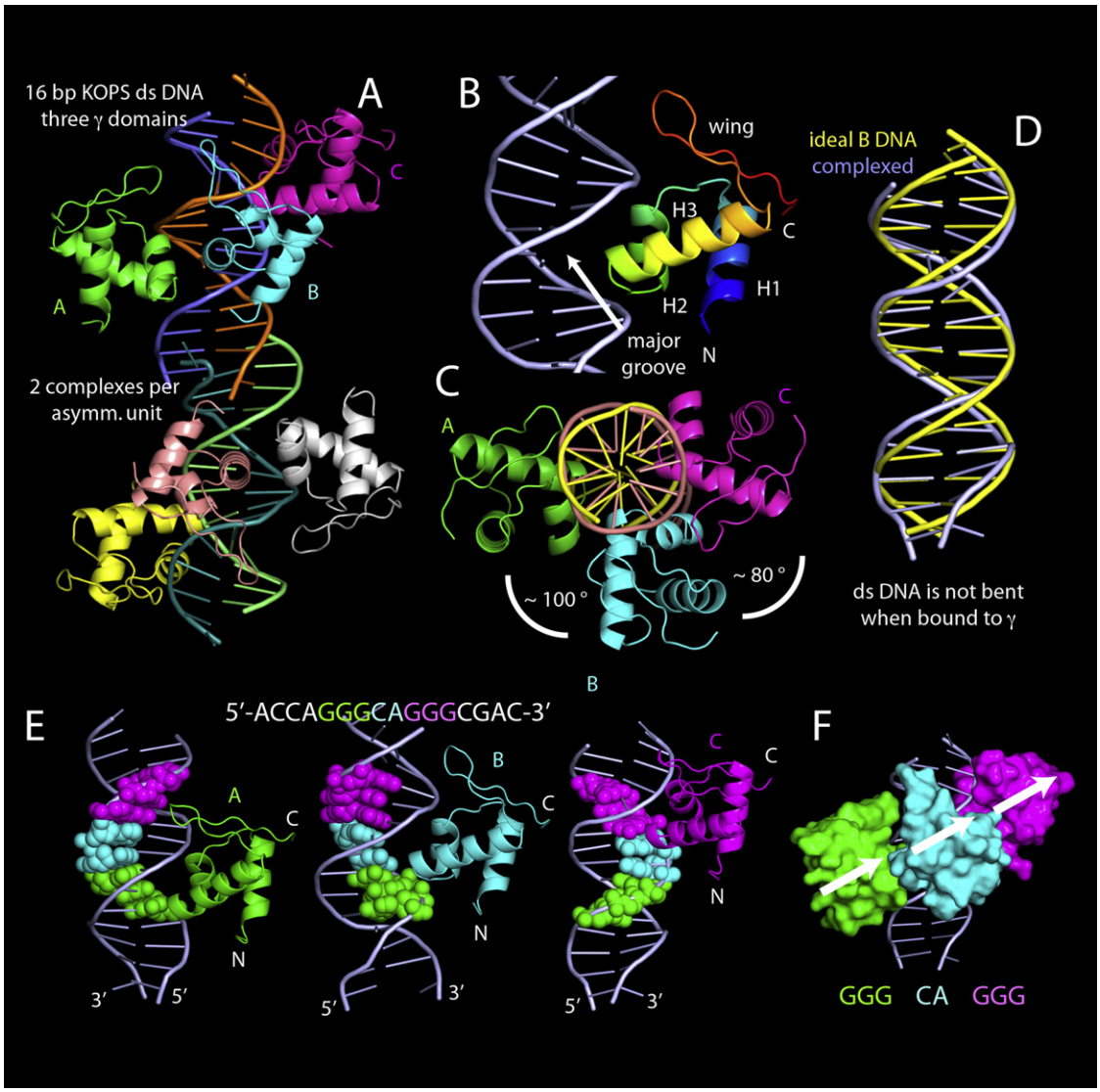

Figure 1. Crystal Structures of the FtsKγ Domain with and without DNA

(A) Cocrystallization of PaFtsKγ with the KOPS-containing DNA duplex 5′-ACCAGGGCAGGGCGAC-3′ (KOPS: GGGCAGGG) produced a structure containing three PaFtsKγ domains bound to double-stranded DNA. The asymmetric unit of these crystals contains two complete complexes. Protein chains A, B, and C are bound to the first duplex; chains D, E, and F are bound to the second.

(B) In the complex, the winged helix domains insert with the loop between H2 and H3 into the major groove of the DNA. The wing, as is common for WHD domains, interacts with the minor groove of the DNA.

(C) The three PaFtsKγ domains are arranged along the DNA to follow the major groove, leading to an arrangement in which they are ~90 degrees apart when looking along the axis of the DNA (A to B: ~100°, B to C: ~80°).

(D) When superimposing the PaFtsKγ-complexed DNA duplex with ideal B DNA, it becomes clear that the DNA is not, or is only very slightly, bent from straight.

(E) The three PaFtsKγ subunits together recognize the GGGCAGGG KOPS motif. Chains A and C recognize a GGG triplet, whereas chain B slots in between the two and recognizes mostly the CA duplet, although very few direct contacts exist, explaining the lack of conservation of the middle bases of the KOPS canonical sequence. The binding mode for chains A and C is very similar, with a tight interaction of the wing with the minor groove. Chain B is tilted and binds in a slightly different way, as expected, because it recognizes a different DNA sequence despite being the same protein.

(F) The recognition of different stretches of DNA by the same domain is possible because the three subunits also interact with themselves. They all bind in the same overall orientation to the DNA, though chain B is slightly tilted.

displaced from DNA as translocation proceeds. Currently, we have no direct evidence that this is possible.

Previously, overlapping triple-KOPS sites were used for biochemical assays involving FtsKγ domain KOPS recognition: GGGCAGGGCAGGGCAGGG. With our structure in hand, the effectiveness of this sequence is readily explained: on the DNA, the γ domains recognize GGG and CA in an alternating way with the binding modes of subunits A (or C) and B following each other along the major groove, providing potential binding sites for all six γ domains, hence enhancing recognition: ABABAB.

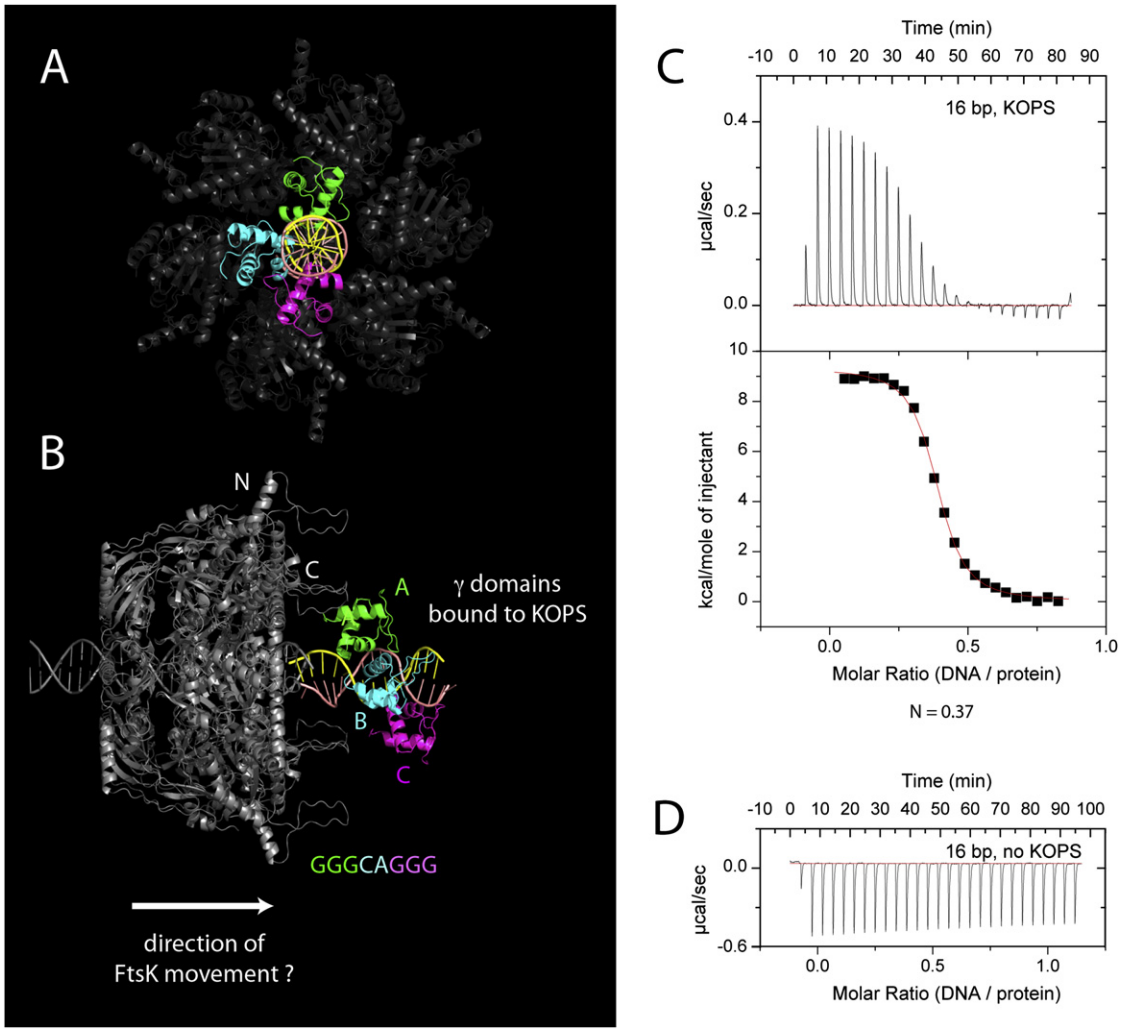

Figure 2. Model of the Motor and FtsKγ Domains onto DNA

(A) When modeling the KOPS:PaFtsKγ complex onto the motor domain (PaFtsK αβ) (Massey et al., 2006), it becomes clear that the γ domains do not follow the 60° rotational repeat of the motor domains.

(B) Using the same model, a prediction can be made for the direction of the motor domain hexamer on KOPS-containing DNA. The model was generated by placing the N termini of the γ domains close to the C termini of the motor domains (Massey et al., 2006). The two parts of the molecules are joined by a linker of 14 amino acids in the full-length protein that are missing between the two structures. This then places the KOPS sequence in a way that the permissive direction of the KOPS sequence goes from left to right. This means that it is likely that the motor complex moves the DNA from the wider end of the cone to the narrower end where the N-terminal α domains are located, as is indicated.

(C) An isothermal titration calorimetry (ITC) experiment shows that three PaFtsKγ domains bind to one KOPS, N = 0.37 (0.33 for 1:3).

(D) Control ITC experiment using double-stranded DNA of the same length without KOPS. No binding is observed.

A Recombination Assay Dependent upon FtsK Loading

In vivo, FtsK translocates DNA until it reaches the *dif* site, whereupon it interacts with XerD to stimulate recombination with a partner *dif* site. Recombination can, therefore, be used as a readout for FtsK translocation up to a *dif* site in vitro, using the soluble derivative $FtsK_{50C}$, consisting of 50 amino acids from $FtsK_N$ fused to $FtsK_C$ (Aussel et al., 2002). In vitro, $FtsK_{50C}$ can stimulate recombination between two *dif* sites provided it can load upon one or the other substrate; one of the *dif* sites can be upon a short DNA that has no potential to allow FtsK to bind as long as the partner *dif* site has a sufficient extra DNA to allow loading on the XerD side of *dif* (Massey et al., 2004). When the XerD side arm is below 50 bp in length, recombination becomes inefficient. The length requirement of the longer substrate can be further reduced by including three copies of KOPS in tandem repeat in addition to a short ≥20 bp arm (Bigot et al., 2006). This led to the proposal that KOPS can act as loading sequences for FtsK. To investigate the requirements of the FtsKγ-KOPS interaction in loading a hexamer of FtsK, this assay was adapted and made more stringent by including a single KOPS sequence separated 5 bp from *dif*, followed by a further 25 bp upon which the hexamer could be loaded, so that FtsK would subsequently

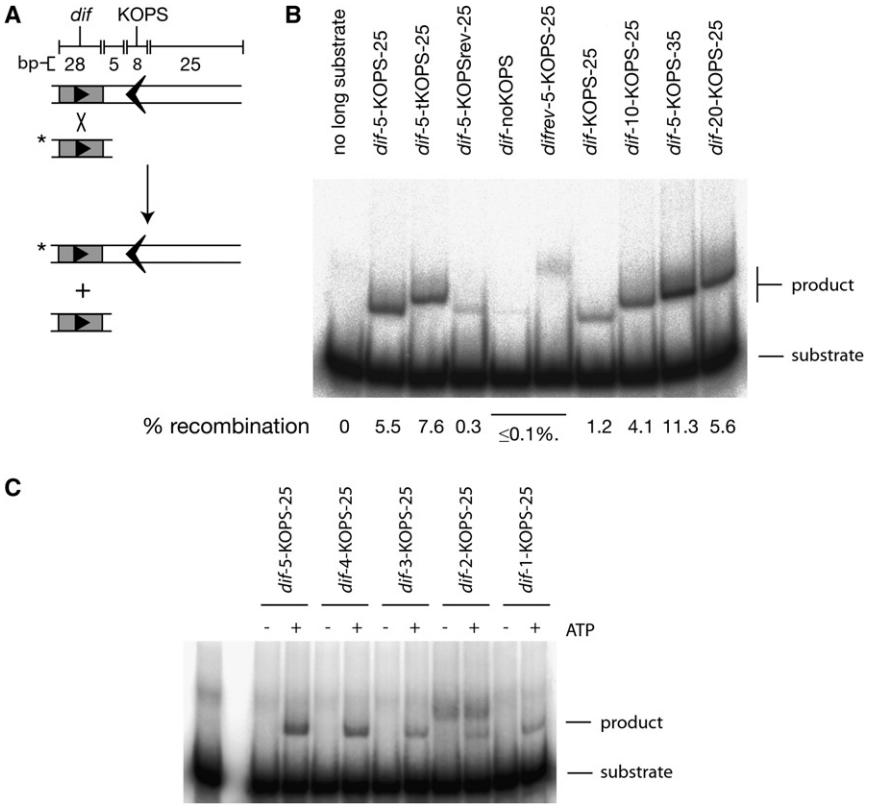

Figure 3. A Recombination Reaction Dependent upon FtsK Loading at KOPS

(A) Schematic diagram of recombination substrates. The *dif* site, present on both substrates, is shown as a gray box containing a triangle, and KOPS is shown as an arrow on the DNA that points in the permissive direction. Presence of a radioactive label is shown by the asterisk. Each longer substrate is named according to the order of its component parts. For example, the substrate shown in (A) is *dif*-5-KOPS-25, where 5 and 25 represent the length of duplex DNA (bp) in these positions. This nomenclature is used for all the subsequent substrates. In this substrate, the XerD binding site of *dif* is closest to KOPS.

(B) Autoradiogram of a recombination gel. Each lane contained XerCD, $FtsK_{50C}$, ATP, and the indicated substrates. The percent recombination shown below each lane is an average derived from two independent experiments using the same conditions. When the level of recombination was too low to quantify, it is indicated as ≤0.1%.

(C) Recombination is dependent upon ATP. Recombination reactions carried out on the indicated substrates in the presence or absence of ATP as indicated.

The smeary band seen in the *difrev*-5-KOPS-25 lane in (B) and the similar bands in the *dif*-2-KOPS-25 lanes in (C) are background bands and unrelated to recombination since they appear with these substrates in the absence of protein.

translocate toward *dif* (Figures 3A and 3B). Recombination on this substrate was efficient. When KOPS was inverted with respect to *dif* (*dif*-5-revKOPS-25) or *dif* inverted with respect to KOPS (*difrev*-5-KOPS-25), recombination was greatly reduced. Similarly, recombination on a substrate of the same length but with no KOPS present was inefficient (*dif*-5-noKOPS-25). Increasing the spacing between *dif* and KOPS had very little effect on the recombination level observed. Lengthening the DNA the other side of KOPS (the site of hexamer loading) to 35 bp led to an increase in recombination, as did including an overlapping triple-KOPS sequence (above), presumably as a result of increased loading efficiency. These findings are in good agreement with the model proposed in Figure 2B for the direction of loading of a FtsK hexamer upon interaction with KOPS.

This assay provides a good test for efficiency of loading of a $FtsK_{50C}$ hexamer at KOPS, as recombination is essentially dependent upon being able to recognize KOPS and load onto the DNA arm such that $FtsK_{50C}$ now translocates toward *dif*.

Recombination Is Dependent upon ATP Hydrolysis

It was clear from the assay shown in Figures 3A and 3B that the presence of a KOPS site acted to load FtsK onto a substrate too short for spontaneous loading to occur with any reasonable efficiency. Since three FtsKγ domains bind to KOPS (Figure 1), it is probable that these nucleate the formation of a hexamer around the DNA. γ-KOPS binding should be a nucleotide-independent event, yielding a loaded hexamer with three γ domains engaged on KOPS and potentially three free γ domains per hexamer. Hexamerization of FtsKαβ has also previously been observed independently of nucleotide (Massey et al., 2006) and is also demonstrated later (Figure 4B). Therefore, we examined the possibility that a hexamer of $FtsK_{50C}$ could simultaneously bind to KOPS and interact with XerD via its free γ domains to stimulate recombination in a nucleotide-independent reaction. To this end, the distance between the KOPS loading site and the *dif* site was reduced in single bp steps, as shown in Figure 3C, and reactions were carried out either with or without addition of ATP. As the KOPS site was moved closer to *dif*, the efficiency of recombination with ATP present declined. Without ATP, none of the substrates showed any detectable recombination. Substituting ATP with either ADPNP, a nonhydrolyzable analog of ATP, or with ADP also failed to give detectable recombination (data not shown). Further, addition of ATPγS, which is slowly hydrolyzed by FtsK and is capable of supporting a low level of recombination on plasmid substrates (Ip et al., 2003) and long linear substrates (Massey et al., 2004), also failed to stimulate recombination in this assay (data not shown). Thus, ATP hydrolysis appears to be necessary for recombination to occur, although we cannot formally exclude that ATPγS inhibits something other than hydrolysis. Substrates with 5 bp between *dif* and KOPS were constructed with a nick in either the top or bottom strand or a single base gap in this spacer region to allow greater flexibility of the complex. Each of these substrates gave recombination products only when ATP was added to the reaction (data not shown). Therefore, a hexamer of FtsK cannot simultaneously bind to KOPS and interact with XerD to stimulate recombination at an adjacent *dif* site. We interpret this to mean that FtsK needs to actively translocate, displacing γ from KOPS, before interaction

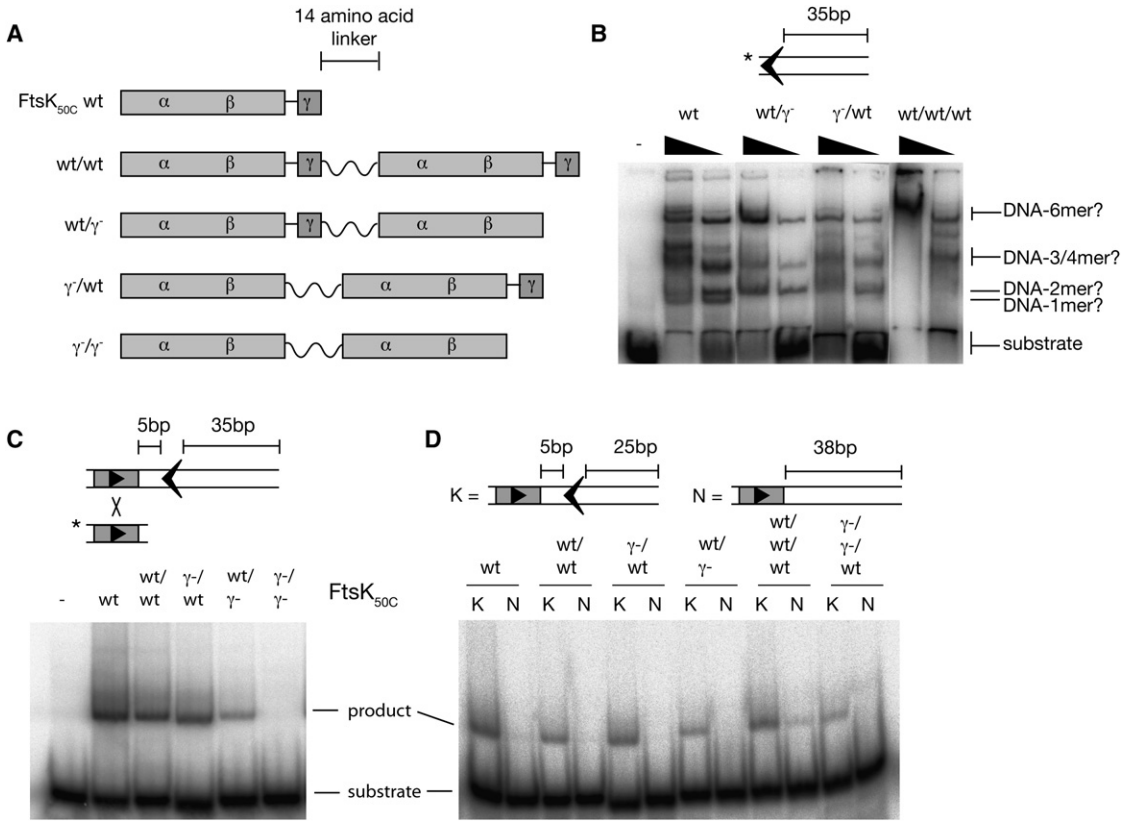

Figure 4. Three γ Domains in a Hexamer Are Sufficient for KOPS-Dependent Recombination

(A) Schematic representation of the covalent dimers of $FtsK_{50C}$ and their indicated nomenclature.

(B) DNA binding of monomeric and covalent dimeric/trimeric $FtsK_{50C}$ derivatives. The substrate is shown schematically above the gel. The KOPS site is flanked by 1 bp to one side and by 35 bp on the other side, upon which FtsK could load. The complexes are putatively identified on the right; the smallest complex, present with $FtsK_{50C}$ but absent in the covalent dimer, is, thus, assigned to be a monomer bound to DNA. Similarly, the smallest complex with the covalent dimer, absent with the trimer, is assigned as a single dimer bound to DNA. The largest complex, common to all the proteins tested, is presumed to be a hexamer and is marked as such. There is no indication that the covalent multimers form higher-order complexes of different composition than monomeric $FtsK_{50C}$.

(C) Recombination activity of the covalent dimeric proteins. Each dimeric protein was active except the γ−/γ− variant.

(D) Comparison of recombination efficiency on substrates of identical length, K, with KOPS, and N, without KOPS. This confirms that the dimeric proteins retain the dependence on KOPS for efficient recombination.

with XerD takes place. It is hard to envisage how ATP hydrolysis by FtsK could activate recombination when the γ-KOPS interaction is intact. Translocation could simply move FtsK into the correct position to interact with XerD. Alternatively, there may be a change in either protein or DNA commensurate with translocation or ATP hydrolysis, which is necessary for recombination stimulation.

Covalent Dimers and Trimers of $FtsK_{50C}$ Are Active In Vivo and In Vitro

A recombinant gene that encodes a covalently linked dimer of $FtsK_{50C}$ containing two copies of $FtsK_{50C}$ separated by a 14 amino acid glycine-rich linker (amino acid sequence GGGSEGGGSEGGSG) allowed the reconstitution of hexamers with six, three, or zero γ domains (Figure 4A). The short linker still supports hexamer formation as depicted in Figure 2B since the N and C termini are close in space (Massey et al., 2006).

Binding of the covalent fusion proteins to a short DNA fragment containing KOPS was compared to that of the monomeric form (Figure 4B). Each of the proteins gave defined complexes on DNA, with the lowest mobility complex being the same for all the variants (Figure 4B). We interpret this complex to be a hexamer loaded onto the DNA. Each of the complexes produced by the covalent fusion proteins was also observed using monomeric $FtsK_{50C}$. There was no evidence for formation of higher-order complexes or aberrant multimerization using the covalent fusion proteins. Therefore, we believe that the covalent fusions are, indeed, capable of forming hexameric rings and do not readily form other higher-order structures. Although other interpretations of the data presented are possible, we believe that this is both the most parsimonious and plausible one. Further, at high-protein concentration, monomeric $FtsK_{50C}$ and the covalent dimeric proteins yielded complexes of the same size when analyzed by gel filtration chromatography (data not shown). The complex was very large and, thus, poorly resolved by this technique but was consistent with being a hexameric ring.

Trimeric forms were also constructed with two copies of the 14 amino acid linker, each flanked by a unique restriction site,

separating the three copies of the $FtsK_{50C}$ monomers. They are described using the nomenclature of Figure 4A. Each of these proteins was tested for the ability to stimulate recombination on a plasmid substrate in vivo. The relevant expression plasmid was transformed into cells harboring a reporter plasmid with two *dif* sites, either without KOPS (KOPS-0) or with each site flanked by nonpermissive KOPS (KOPS-2) (Sivanathan et al., 2006), and deletion reactions were studied over time after induction of the dimeric $FtsK_{50C}$ derivatives. A plasmid expressing monomeric $FtsK_{50C}$ was used alongside for comparison (data not shown). The WT/WT and γ−/WT dimers each showed robust recombination stimulation in vivo on the KOPS-0 substrate, but the WT/γ− dimer showed very low activity. As expected, the γ−/γ− dimer was incompetent for activating recombination. Recombination on these plasmid substrates confirms that three γ domains per hexamer are sufficient to stimulate recombination. Each of the constructs showed a reduced level of recombination on the KOPS-2 substrate compared to KOPS-0, suggesting that the covalent dimers were able to respond to the presence of KOPS as monomeric $FtsK_{50C}$ did. A covalent trimeric WT/WT/WT protein also stimulated recombination. No recombination was observed upon expression of the γ−/γ−/γ− protein, but γ−/γ−/WT did show a low level of activity (data not shown).

Three γ Domains per Hexamer Are Sufficient to Load at KOPS

Each of the dimeric proteins was purified and tested for ATPase activity in vitro. Protein concentrations were adjusted so that the same concentration of active sites was present in each assay, and each of the dimeric proteins appeared to be at least as active as a similar preparation of monomeric $FtsK_{50C}$ (data not shown).

The dimeric forms of $FtsK_{50C}$ were tested in the previously described recombination reaction dependent upon loading at KOPS to be able to recombine two short DNA fragments. With normalized protein concentrations, each of the dimers was again seen to be active in this assay, apart from the γ−/γ− dimer (Figure 4C). Therefore, hexamers with three or six γ domains were able to bind to these substrates containing KOPS and subsequently activate recombination.

In order to test whether the dimeric forms of the protein had a similar requirement for KOPS in order to load onto a short DNA arm, each of the proteins was tested on substrates of the same length either with or without a KOPS site (Figure 4D). This confirmed that the loading of the dimers onto these substrates was still KOPS dependent and that, in the absence of KOPS, no recombination was observed. When a similar experiment was carried out for the trimeric variants of $FtsK_{50C}$, it was observed that both the WT/WT/WT and γ−/γ−/WT trimers were active when KOPS was present, but the WT/WT/WT trimer also showed a low level of activity on the "no KOPS" substrate, demonstrating that, at least in the trimeric form of the protein, some of the dependence upon loading by KOPS could be overcome. The trimeric form of $FtsK_{50C}$ would be expected to form hexamers more readily on DNA than a monomeric form because interaction between two molecules in the trimeric form is all that is required. Perhaps this relaxed requirement for hexamer formation is what allows the γ−/γ−/WT trimer to load at KOPS despite having only two γ domains per hexamer.

KOPS Acts as a Loading Site for FtsK and Is Not Recognized in the Nonpermissive Orientation

It is clear that KOPS can act as a loading site for FtsK, but it has been previously proposed that translocating FtsK also recognizes KOPS in the opposite nonpermissive orientation and uses this as a signal to stop translocation and perhaps even reverse its direction of translocation (Bigot et al., 2005, 2006; Pease et al., 2005; Ptacin et al., 2006; Saleh et al., 2005). However, such a recognition of KOPS would require either that the γ domains bind KOPS in a different mode to that shown in Figure 1 or that the linker between β and γ is sufficiently long and flexible enough to stretch over the γ-KOPS complex and maintain the same binding mode. However, both of these possibilities seem unlikely, given our structural data. Alternatively, we propose that KOPS is simply an efficient loading site for FtsK and that, when sufficient protein is used, the majority of KOPS sites will be occupied by FtsK. In order to test these different possibilities, the loading-dependent recombination assay previously used was altered such that a KOPS sequence was inserted in the opposite orientation between the permissive KOPS loading site and the *dif* site (Figures 5A–5C). The distance between *dif* and the inserted KOPS site was then varied; if γ can recognize nonpermissive KOPS, then this distance should be inconsequential. However, if pausing requires loading of FtsK at the reversed site, then this will become more efficient when there is more DNA upon which to load, and, thus, the reversed KOPS site should be a better block as the distance increases.

Recombination reactions using these substrates showed that, when the opposing KOPS site was placed just 5 bp from the *dif* site, the recombination efficiency was not lowered when compared to a control substrate of similar length (*dif*-20-KOPS-25) (Figures 5B and 5C). As the distance between the reversed KOPS and *dif* was increased, the recombination rate concurrently decreased. Indeed, when the distance was increased to 30 bp, recombination was barely detectable. Recombination reactions using various short time points confirmed that there was no difference in recombination rate between the control substrate without KOPS and the substrate with KOPS 5 bp from *dif* (Figure 5C). Therefore, we conclude that translocating FtsK does not respond to a reversed KOPS sequence, and, hence, FtsKγ recognizes KOPS in only one direction.

Concluding Remarks

KOPS-directed FtsK translocation on the *E. coli* chromosome localizes the sister *dif* sites to the septum. Thereupon, FtsK stimulates chromosome unlinking by XerCD recombination. The first experiments that addressed the directional translocation of FtsK were interpreted as FtsK stopping translocation at nonpermissive KOPS and then sometimes reversing the translocation direction (Bigot et al., 2005, 2006; Pease et al., 2005; Ptacin et al., 2006; Saleh et al., 2005). It was inferred that FtsK translocated through permissive KOPS. Subsequently, it was proposed that permissive KOPS could also act as a loading site for FtsK and thereby facilitate directional translocation (Bigot et al., 2006; Sivanathan et al., 2006). This dual action would require

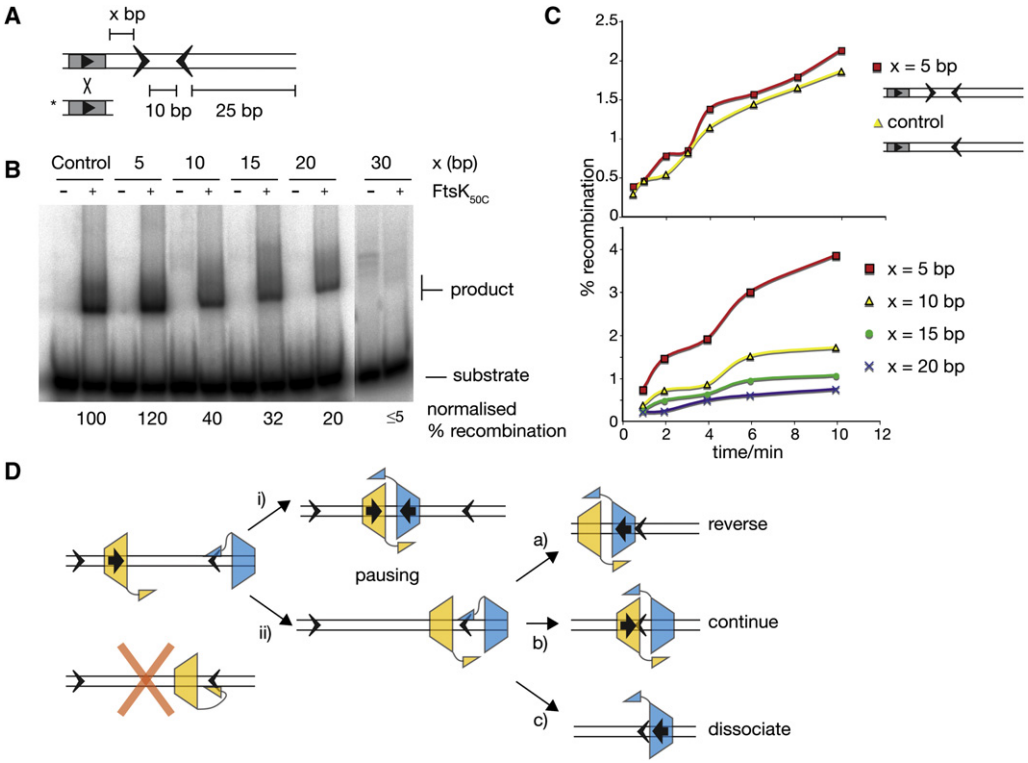

Figure 5. FtsK Cannot Recognize KOPS in the Reverse Direction

(A) Schematic representation of the substrates used. Nomenclature is as in Figure 3. In these substrates, a second (nonpermissive) KOPS is added between the *dif* site and the KOPS loading site. An "x" represents the distance in bp between *dif* and this additional KOPS.

(B) Recombination reactions using substrates with a reversed KOPS. The control is *dif*-20-KOPS-25, used previously (Figure 3), which is a similar length to the other substrates here. The quantified percentage of recombination from each substrate is shown below the autoradiograph and is normalized to the control reaction. Multiple repeats of this experiment give the same trends.

(C) Graphs showing recombination against time for the substrates shown in (B). The top panel compares the control substrate with the substrate having reversed KOPS 5 bp from *dif*. The lower panel shows the effect of varying this distance between *dif* and the reversed KOPS. Again, a representative set of data is shown, but repeats give similar trends.

(D) Model for collision of FtsK hexamers following directional KOPS loading. Each hexamer is represented as a cone on the DNA, and, for clarity, only a single γ domain is shown as a connected triangle. Since γ binds KOPS in a specific orientation (Figure 1), recognition of an inverted KOPS would require the linker between the motor and γ to loop over the entire length of the γ-KOPS complex. This is disallowed (red cross). Thus, FtsK is never loaded in the "wrong" orientation, nor can it recognize an inverted KOPS during translocation. Translocating hexamers have a black arrow to show their movement relative to the DNA. Initially, both hexamers are loaded directionally at KOPS, and the yellow hexamer has begun translocation. In scheme (Di), both hexamers translocate and collide in the intervening DNA. In (Dii), one hexamer remains bound at KOPS. Both schemes could result in pausing of translocation upon collision. The various subsequent outcomes are then shown (Da)–(Dc), with (arbitrary) reference to the initially translocating hexamer: in (Da) and (Db), one motor pushes the other, whereas in (Dc), one motor dissociates and the other is free to translocate.

different binding modes to KOPS with different mechanistic outcomes: stalling at reversed KOPS would need recognition in a way that would lead to downregulation of the motor, and loading at permissive KOPS would require that the motor be translocation competent.

Based on the structures and the biochemical data showing that translocating FtsK does not respond to nonpermissive KOPS, we propose a model whereby KOPS acts solely to orient the direction of the FtsK hexamer on DNA at the initial binding event. Three γ domains of a FtsK hexamer bind to KOPS simultaneously and are sufficient for a hexamer to be loaded on the DNA "upstream" of KOPS. This mechanism requires no obligatory regulation of motor activity upon KOPS binding. If KOPS is simply a directional loading site that promotes formation of a hexamer specifically on DNA, then it may be expected that FtsK variants that form hexamers more readily around DNA would be able to show some KOPS-independent activity, as, indeed, appears to be the case for the covalent trimers of FtsK.

We propose that the observed pausing and reversal of FtsK upon encounter of KOPS in the nonpermissive orientation is not a consequence of recognition of this KOPS by the translocating FtsK. Rather, it results from efficient loading of a second FtsK hexamer at KOPS, which would be oriented opposite to the direction of translocation of the first. Therefore, a head-on collision between the two FtsK hexamers is envisaged (Figure 5D). This could then lead to pausing; either the translocating hexamer is stopped by encounter of the FtsKγ-KOPS complex, or it displaces γ from KOPS and is stopped by encounter with the newly freed motor of the second hexamer. Indeed, head-to-head hexamers have been seen in both crystal

structures and EM images (Massey et al., 2006). Subsequently, either one or the other hexamer could dissociate, leaving the remaining one free to translocate, or both could remain engaged on DNA but one could successfully push the other (Figure 5D). The outcome of this collision may be biased toward one pathway as a result of one hexamer being associated with KOPS. Further, because the binding energy of three γ domains to KOPS is similar to that released upon hydrolysis of ATP, it is possible that FtsK overcoming this barrier may be a relatively slow event compared to translocation events at speeds of ~5 kbsec^{-1} (Pease et al., 2005). The result of this would be that the majority of observed collisions would be at KOPS rather than on the intervening DNA.

In conclusion, we believe that all previous data are consistent with this interpretation of KOPS acting simply as a loading site and that an FtsK hexamer is a unidirectional, hexameric DNA translocase. The biological consequence of directional loading of FtsK by KOPS is that translocation will be toward the *dif* site from either side and will result in FtsK encountering the recombinases XerCD at *dif* to stimulate their recombination activity. A similar model of directional loading can be expanded to other members of the FtsK/SpoIIIE family to explain the polarized movement of a motor on a chromosome.

EXPERIMENTAL PROCEDURES

Cloning, Expression, and Purification of PaFtsK γ Domain

Pseudomonas aeruginosa FtsK (Uniprot:FTSK_PSEAE) γ domain was expressed as described before (Sivanathan et al., 2006). Seleno-methionine-substituted protein was produced using published methods (van den Ent et al., 1999), and 5 mM reducing agent (β-mercaptoethanol for nickel chromatography and DTT for all others) was used in all buffers.

Crystal Structure of PaFtsKγ

Initial crystallization conditions were found using our 100 nl plus 100 nl high-throughput crystallization facility (Stock et al., 2005). Diffracting crystals were produced by sitting drop vapor diffusion in MRC 96-well crystallization plates mixing 500 nl plus 500 nl of protein (9 mg/ml) and crystallization solution. Crystallization solution was 100 mM Tris/HCl, pH 7.0, 30% (v/v) PEG 300, and 14.3% (w/v) PEG 1000. A crystal without additional cryo protection was used for data collection on beamline ID14eh4 (ESRF, Grenoble, France). The structure was solved by molecular replacement using our previous NMR structure as a template (PDB ID 2J5O). The program PHASER (McCoy et al., 2007) placed eight molecules in the asymmetric unit. The structure was built using MAIN (Turk, 1992) and refined using REFMAC5 (Murshudov et al., 1997). See Table 2 for refinement statistics to 1.4 Å resolution.

Crystal Structure of PaFtsKγ in Complex with KOPS-Containing ds DNA

KOPS1 ds DNA was obtained in PAGE-purified form from Operon (UK) and annealed without further purification: 5′-ACCAGGGCAGGGCGAC-3′ and 5′-GTCGCCCTGCCCTGGT-3′. Initial crystallization conditions were found using high-throughput crystallization as above (Stock et al., 2005). Diffracting crystals were produced by sitting drop vapor diffusion in MRC 96-well crystallization plates mixing 200 + 200 nl of protein and crystallization solution. Protein solution contained 13 mg/ml SeMet-substituted PaFtsKγ plus 13 mg/ml ds KOPS1 DNA. Crystallization solution was 200 mM citric acid/NaOH pH 3.5 and 29% (w/v) PEG 6000. A three-wavelength SeMet MAD data set was collected on beamline ID14eh4 (ESRF, Grenoble, France) without any additional cryoprotection. See Table 1 for data collection details. The structure was solved de novo using SHELXD (Schneider and Sheldrick, 2002) and SHARP (Bricogne et al., 2003), built with MAIN (Turk, 1992), and refined using CNS (Brunger et al., 1998). The asymmetric unit contains two complexes consisting of ds KOPS1 DNA and three PaFtsKγ domains. See Table 2 for refinement statistics to 1.9 Å.

Isothermal Titration Calorimetry of the PaFtsKγ:KOPS Interaction

The experiments were performed on a VP-ITC micro calorimeter from MicroCal (UK) at 10°C. Protein and DNAs were in 20 mM Tris/HCl, 1 mM EDTA, 1 mM Na azide, (pH 7.5). PaFtsKγ was in the cuvette (2 ml at 100 μM), and KOPS1 ds DNA was added in 5 μl steps (500 μl at 1 mM). Delay was 210 s and stirrer speed 300. If the complex has a 1:3 stoichiometry, as predicted from the crystal structure, binding should be complete after 2000 μl / 5 μl / (1 mM / 0.1 mM × 3) = 13.3 steps. This can, indeed, be seen in Figure 2C. As a control, non-KOPS-containing ds DNA of the same length (5′-TGTTTCACGGGAAACA-3′) was added. A single-site model was fitted for obtaining the stoichiometry.

Cloning Linked Dimeric Proteins

$FtsK_{50C}$ was amplified by PCR using primers, as outlined in the Supplemental Data. The PCR products were cloned into pBAD24 so that two copies of $FtsK_{50C}$ were separated by a 42 base linker, and the dimeric protein was expressed under the control of the arabinose promoter. Constructs lacking one or the other γ domain were produced by PCR and cloned as above. Trimeric proteins were constructed using a similar strategy. Each construct was sequenced to confirm that there were no unexpected mutations introduced by PCR.

Protein Purification for Biochemical Assays

A $\Delta FtsK_C$ strain of *E. coli* (DS9041) carrying the relevant expression plasmid was grown to an OD_{600} of ~0.8. Induction was with 0.2% arabinose for 1 hr. Cells were harvested and then lysed in buffer A: 50 mM HEPES (pH 8.0), 250 mM NaCl, 10% glycerol, and 0.01% Triton X-100. Cell debris was removed by centrifugation at 40,000 g, and the resulting supernatant was applied to TALON resin (Clonetech). The resin was washed using buffer B: 50 mM HEPES (pH 8.0), 250 mM NaCl, 5% glycerol, 5 mM imidazole until the wash had no significant absorbance at 280 nm. Protein was eluted using buffer A supplemented with 250 mM imidazole, aliquoted, and stored at −20°C until use.

Recombination Reactions

In vitro recombination reactions contained 25 mM Tris/HCl pH 7.5, 10 mM $MgCl_2$, 1 nM radiolabeled short *dif* fragment, 10 nM longer *dif*- KOPS fragment, 150 nM XerC, 30 nM XerD, and, subsequently, 40 nM $FtsK_{50C}$ hexamer was added, whether it be made up of monomeric or dimeric/trimeric subunits. After 2 min at room temperature, 2 mM ATP was added unless stated otherwise, and reactions were placed at 37°C for 30 min unless specified. Reactions were stopped by addition of 0.1% SDS and 0.1 mg/ml proteinase K and electrophoresed through 7% acrylamide containing 0.1% SDS in 1 × TBE buffer (90 mM Tris-borate, 1 mM EDTA). Gels were dried and imaged using a Fuji FLA-3000 scanner and ImageGauge software. Oligonucleotide sequences of the various DNA substrates are in the Supplemental Data. Recombination assays in vivo were as described in Sivanathan et al., 2006.

DNA-Binding Assays

Reactions contained 25 mM Tris/HCl pH 7.5, 5% glycerol, 1 nM labeled 1-KOPS-35 ds DNA. Each protein tested was used at both 200 and 40 nM $FtsK_{50C}$ hexamer equivalent. Reactions were electrophoresed through 7% acrylamide in 0.5 × TBE buffer and imaged as above.

ACCESSION NUMBERS

Coordinates of FTsKγ and FtsKγ:KOPS DNA have been deposited in the Protein Data Bank (PDB) with accession codes 2VE8 and 2VE9, respectively.

SUPPLEMENTAL DATA

The Supplemental Data include two figures and one table and can be found with this article online at http://www.molecule.org/cgi/content/full/31/4/498/DC1/.

ACKNOWLEDGMENTS

Diffraction data were collected at beamline ID14eh4 at the ESRF (Grenoble, France), and we would like to thank the beamline staff for excellent support. We would like to thank Eva Schmid (LMB, Cambridge) for help with the ITC experiment. This research was supported by the Wellcome Trust.

Received: December 20, 2007
Revised: March 10, 2008
Accepted: May 29, 2008
Published: August 21, 2008

REFERENCES

Aussel, L., Barre, F.X., Aroyo, M., Stasiak, A., Stasiak, A.Z., and Sherratt, D. (2002). FtsK is a DNA motor protein that activates chromosome dimer resolution by switching the catalytic state of the XerC and XerD recombinases. Cell *108*, 195–205.

Bath, J., Wu, L.J., Errington, J., and Wang, J.C. (2000). Role of Bacillus subtilis SpoIIIE in DNA transport across the mother cell-prespore division septum. Science *290*, 995–997.

Bigot, S., Corre, J., Louarn, J.M., Cornet, F., and Barre, F.X. (2004). FtsK activities in Xer recombination, DNA mobilization and cell division involve overlapping and separate domains of the protein. Mol. Microbiol. *54*, 876–886.

Bigot, S., Saleh, O.A., Lesterlin, C., Pages, C., El Karoui, M., Dennis, C., Grigoriev, M., Allemand, J.F., Barre, F.X., and Cornet, F. (2005). KOPS: DNA motifs that control E. coli chromosome segregation by orienting the FtsK translocase. EMBO J. *24*, 3770–3780.

Bigot, S., Saleh, O.A., Cornet, F., Allemand, J.F., and Barre, F.X. (2006). Oriented loading of FtsK on KOPS. Nat. Struct. Mol. Biol. *13*, 1026–1028.

Bigot, S., Sivanathan, V., Possoz, C., Barre, F.X., and Cornet, F. (2007). FtsK, a literate chromosome segregation machine. Mol. Microbiol. *64*, 1434–1441.

Bricogne, G., Vonrhein, C., Flensburg, C., Schiltz, M., and Paciorek, W. (2003). Generation, representation and flow of phase information in structure determination: recent developments in and around SHARP 2.0. Acta Crystallogr. D Biol. Crystallogr. *59*, 2023–2030.

Brunger, A.T., Adams, P.D., Clore, G.M., DeLano, W.L., Gros, P., Grosse-Kunstleve, R.W., Jiang, J.S., Kuszewski, J., Nilges, M., Pannu, N.S., et al. (1998). Crystallography & NMR system: A new software suite for macromolecular structure determination. Acta Crystallogr. D Biol. Crystallogr. *54*, 905–921.

Corre, J., and Louarn, J.M. (2002). Evidence from terminal recombination gradients that FtsK uses replichore polarity to control chromosome terminus positioning at division in Escherichia coli. J. Bacteriol. *184*, 3801–3807.

Dorazi, R., and Dewar, S.J. (2000). Membrane topology of the N-terminus of the Escherichia coli FtsK division protein. FEBS Lett. *478*, 13–18.

Draper, G.C., and Gober, J.W. (2002). Bacterial chromosome segregation. Annu. Rev. Microbiol. *56*, 567–597.

Ebersbach, G., and Gerdes, K. (2005). Plasmid segregation mechanisms. Annu. Rev. Genet. *39*, 453–479.

Gajiwala, K.S., and Burley, S.K. (2000). Winged helix proteins. Curr. Opin. Struct. Biol. *10*, 110–116.

Ghosh, S.K., Hajra, S., Paek, A., and Jayaram, M. (2006). Mechanisms for chromosome and plasmid segregation. Annu. Rev. Biochem. *75*, 211–241.

Goehring, N.W., and Beckwith, J. (2005). Diverse paths to midcell: assembly of the bacterial cell division machinery. Curr. Biol. *15*, R514–R526.

Grainge, I., Bregu, M., Vazquez, M., Sivanathan, V., Ip, S.C., and Sherratt, D.J. (2007). Unlinking chromosome catenanes in vivo by site-specific recombination. EMBO J. *26*, 4228–4238.

Gunton, J.E., Gilmour, M.W., Baptista, K.P., Lawley, T.D., and Taylor, D.E. (2007). Interaction between the co-inherited TraG coupling protein and the TraJ membrane-associated protein of the H-plasmid conjugative DNA transfer system resembles chromosomal DNA translocases. Microbiology *153*, 428–441.

Hendrickson, H., and Lawrence, J.G. (2006). Selection for chromosome architecture in bacteria. J. Mol. Evol. *62*, 615–629.

Ip, S.C., Bregu, M., Barre, F.X., and Sherratt, D.J. (2003). Decatenation of DNA circles by FtsK-dependent Xer site-specific recombination. EMBO J. *22*, 6399–6407.

Iyer, L.M., Makarova, K.S., Koonin, E.V., and Aravind, L. (2004). Comparative genomics of the FtsK-HerA superfamily of pumping ATPases: implications for the origins of chromosome segregation, cell division and viral capsid packaging. Nucleic Acids Res. *32*, 5260–5279.

Levy, O., Ptacin, J.L., Pease, P.J., Gore, J., Eisen, M.B., Bustamante, C., and Cozzarelli, N.R. (2005). Identification of oligonucleotide sequences that direct the movement of the Escherichia coli FtsK translocase. Proc. Natl. Acad. Sci. USA *102*, 17618–17623.

Liu, N.J., Dutton, R.J., and Pogliano, K. (2006). Evidence that the SpoIIIE DNA translocase participates in membrane fusion during cytokinesis and engulfment. Mol. Microbiol. *59*, 1097–1113.

Massey, T.H., Aussel, L., Barre, F.X., and Sherratt, D.J. (2004). Asymmetric activation of Xer site-specific recombination by FtsK. EMBO Rep. *5*, 399–404.

Massey, T.H., Mercogliano, C.P., Yates, J., Sherratt, D.J., and Löwe, J. (2006). Double-stranded DNA translocation: structure and mechanism of hexameric FtsK. Mol. Cell *23*, 457–469.

McCoy, A.J., Grosse-Kunstleve, R.W., Adams, P.D., Winn, M.D., Storoni, L.C., and Read, R.D. (2007). Phaser crystallographic software. J. Appl. Cryst. *40*, 658–674.

Murshudov, G.N., Vagin, A.A., and Dodson, E.J. (1997). Refinement of macromolecular structures by the maximum-likelihood method. Acta Crystallogr. D Biol. Crystallogr. *53*, 240–255.

Pease, P.J., Levy, O., Cost, G.J., Gore, J., Ptacin, J.L., Sherratt, D., Bustamante, C., and Cozzarelli, N.R. (2005). Sequence-directed DNA translocation by purified FtsK. Science *307*, 586–590.

Ptacin, J.L., Nollmann, M., Bustamante, C., and Cozzarelli, N.R. (2006). Identification of the FtsK sequence-recognition domain. Nat. Struct. Mol. Biol. *13*, 1023–1025.

Saleh, O.A., Perals, C., Barre, F.X., and Allemand, J.F. (2004). Fast, DNA-sequence independent translocation by FtsK in a single-molecule experiment. EMBO J. *23*, 2430–2439.

Saleh, O.A., Bigot, S., Barre, F.X., and Allemand, J.F. (2005). Analysis of DNA supercoil induction by FtsK indicates translocation without groove-tracking. Nat. Struct. Mol. Biol. *12*, 436–440.

Schneider, T.R., and Sheldrick, G.M. (2002). Substructure solution with SHELXD. Acta Crystallogr. D Biol. Crystallogr. *58*, 1772–1779.

Sherratt, D.J. (2003). Bacterial chromosome dynamics. Science *301*, 780–785.

Sivanathan, V., Allen, M.D., de Bekker, C., Baker, R., Arciszewska, L.K., Freund, S.M., Bycroft, M., Löwe, J., and Sherratt, D.J. (2006). The FtsK gamma domain directs oriented DNA translocation by interacting with KOPS. Nat. Struct. Mol. Biol. *13*, 965–972.

Stock, D., Perisic, O., and Lowe, J. (2005). Robotic nanolitre protein crystallisation at the MRC Laboratory of Molecular Biology. Prog. Biophys. Mol. Biol. *88*, 311–327.

Strick, T.R., and Quessada-Vial, A. (2006). FtsK: a groovy helicase. Nat. Struct. Mol. Biol. *13*, 948–950.

Turk, D. (1992). Weiterentwicklung eines Programms für Molekülgrafik und Elektrondichte-Manipulation und seine Anwendung auf verschiedene Protein-Strukturaufklärungen (München: Technische Universität München).

van den Ent, F., Lockhart, A., Kendrick-Jones, J., and Lowe, J. (1999). Crystal structure of the N-terminal domain of MukB: a protein involved in chromosome partitioning. Structure *7*, 1181–1187.

Vicente, M., and Rico, A.I. (2006). The order of the ring: assembly of Escherichia coli cell division components. Mol. Microbiol. *61*, 5–8.

Wu, L.J., Lewis, P.J., Allmansberger, R., Hauser, P.M., and Errington, J. (1995). A conjugation-like mechanism for prespore chromosome partitioning during sporulation in Bacillus subtilis. Genes Dev. *9*, 1316–1326.

Yates, J., Zhekov, I., Baker, R., Eklund, B., Sherratt, D.J., and Arciszewska, L.K. (2006). Dissection of a functional interaction between the DNA translocase, FtsK, and the XerD recombinase. Mol. Microbiol. *59*, 1754–1766.